A Letters Journal Exploring the Frontiers of Physics

September 2014

EPL, **107** (2014) 54001
doi: 10.1209/0295-5075/107/54001

www.epljournal.org

Non-reciprocal transmission of terahertz waves through a photonic crystal cavity with graphene

Yu Zhou, Ye-Qing Dong, Kun Zhang, Ru-Wen Peng[a], Qing Hu and Mu Wang

National Laboratory of Solid State Microstructures and Department of Physics, National Center of Microstructures and Quantum Manipulation, Nanjing University - Nanjing 210093, China

received 19 June 2014; accepted in final form 11 August 2014
published online 26 August 2014

PACS 42.25.Bs – Wave propagation, transmission and absorption
PACS 85.70.Sq – Magnetooptical devices
PACS 78.67.Wj – Optical properties of graphene

Abstract – In this work, we theoretically investigate non-reciprocal propagation of terahertz (THz) waves through a photonic crystal cavity integrated with graphene under external magnetic field. The magnetic field applied perpendicular to the graphene plane introduces an asymmetric conductivity tensor into the system, thus the Jones matrix of THz waves propagating in one direction is not the transpose of the one in the reversal direction. As a consequence, non-reciprocal propagation is achieved in the THz regime, which has been verified by the calculation of non-reciprocal photonic band structures, transmission spectra, and also electrical-field distributions. Further, by tuning the magnetic field or the Fermi level of graphene, such non-reciprocal transmission can be drastically tuned. This tunable non-reciprocity at the level of material response enables us to design photonic structures which can let a specific mode pass but its time-reversal counterpart stop. Moreover, high-performance non-reciprocal features have been found in periodic photonic crystal stacks with graphene. Our investigations may provide a unique approach to guide THz waves and achieve potential applications on one-way devices (*e.g.* isolators) in the THz regime.

Introduction. – The study of reciprocity in wave propagation has a long history. In 1959, De Hoop formulated his reciprocity theorem under the condition that all the materials in electromagnetic scattering problems were characterized by symmetric tensors and were independent of the electric and magnetic fields [1,2]. This means that asymmetry in the material response function, *i.e.* permittivity, permeability, or conductivity may lead to the failure of reciprocity [3–10]. A polarized wave propagating through this kind of asymmetric medium may have different transmission spectra and band structures from its time-reversal counterpart [11–21]. For example, in magneto-optic media, the magnetic field perpendicular to the plane introduces asymmetric off-diagonal terms into the permittivity tensor. In such media, the Jones matrix of one direction is not the transpose of the one in the reverse direction [2], thus the circularly polarized waves have different transmissions depending on its direction. In recent years, there has been an increasing interest in non-reciprocal devices [22–28]. For example, based on gyromagnetic photonic crystals, one-way modes have been successfully achieved in the experiments [22–26]. Non-reciprocal devices such as optical isolators have many applications and have been intensely investigated. Up to now, most of the works concern the traditional magneto-optic materials we mentioned above or nonlinear materials [29,30], and mainly focus on microwave and infrared frequency regions. However, there still lack non-reciprocal devices for THz waves, especially electric tunable ones.

Since the development of the mechanical exfoliation method [31], graphene has been increasingly used in photonics and plasmonics [32,33]. Similarly to magneto-optic materials, graphene possesses an asymmetric conductivity tensor under the magnetic field [34,35]. Therefore, circularly polarized waves may have different transmissions depending on its incident direction, *i.e.* non-reciprocal transmission. What is more, graphene has two advantages over other materials. Firstly, its properties can be easily tuned either by the external magnetic field or the Fermi level. Secondly, it has an electromagnetic response

[a] E-mail: rwpeng@nju.edu.cn (corresponding author)

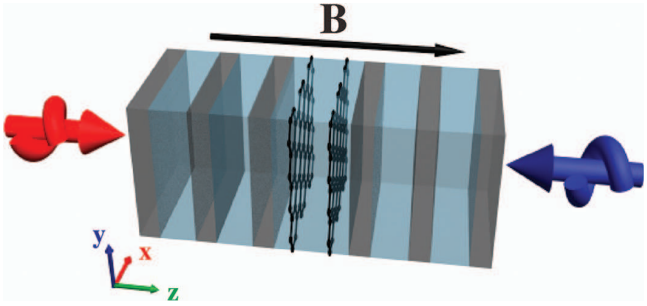

Fig. 1: (Colour on-line) Schematic illustration of the photonic crystal cavity. All the slabs are designed to be quarter-wave plates at 336 μm. Grey and blue slabs are dielectric slabs with permittivity $\varepsilon_1 = 11.7$ and $\varepsilon_2 = 3.8$, respectively. Two graphene layers are located in the centre. The black arrow denotes the external magnetic field along the $+Z$-direction. Two spiral arrows in red and blue indicate the right-handed circularly polarized THz waves propagating forward and backward, respectively.

in a rather broad frequency range, especially in the THz region. In this paper, we have designed a photonic cavity in the THz region with two graphene sheets located in its centre. A magnetic field is applied perpendicularly to the plane to provide the necessary condition for reciprocity breaking. And then the non-reciprocal effect is verified by the calculation of photonic band structures, transmission spectra and electrical-field distributions. By tuning the magnetic field or the Fermi level of graphene, the non-reciprocal transmission can be drastically tuned, which may provide an approach to design active non-reciprocal devices in the THz region. Moreover, high-performance non-reciprocal features have also been found in periodic photonic crystal stacks with graphene.

Theoretical model. – We begin with designing a cavity consisting of three photonic crystal unit cells mirroring itself, as shown in fig. 1. Grey and blue slabs are dielectric slabs with permittivity $\varepsilon_1 = 11.7$ and $\varepsilon_2 = 3.8$, respectively. All the slabs are designed to be quarter-wave plates at 336 μm. The centre of the cavity is made by two quarter-wave slabs with the same refractive index $\varepsilon_2 = 3.8$ each of which has one graphene sheet located at the centre. Under magnetic field, graphene possesses Hall conductivity. The 2D conductivity of graphene is now an asymmetric tensor which only depends on the direction of the external magnetic field, regardless of the waves propagating therein. This would lead to reciprocity failure. Such reciprocity failure can be directly demonstrated by the calculation of transmission spectra which would be different depending on propagating directions (forward or backward).

To calculate the transmission spectra in such system, the S-matrix approach [4,6] is extended into a vector form for the consideration of Hall conductivity which will mix x and y polarizations. In this paper, spatial dispersion is neglected because we focus on the low THz frequency region [35]. The graphene is treated as an infinitesimally thin conductive layer which has a 2D conductivity tensor:

$$\sigma = \begin{pmatrix} \sigma_{xx} & \sigma_{xy} \\ \sigma_{yx} & \sigma_{yy} \end{pmatrix} = \begin{pmatrix} \sigma_l & \sigma_h \\ -\sigma_h & \sigma_l \end{pmatrix}, \tag{1}$$

where σ_l and σ_h are longitudinal and Hall conductivities of the graphene, respectively. Two diagonal terms are identical while two off-diagonal terms have opposite signs. It is apparent that the 2D conductivity is asymmetric and independent of the propagation direction of the incident waves. In the calculation, the temperature is set to be 300 K. All the conductivity values are calculated using the formula in ref. [34]. Scattering effects in graphene are taken into account by setting the imaginary part of energy to 6.8 meV. Slight changes of these parameters will not affect the results.

We choose two tangential components of the electric field E_x and E_y as independent variables. Then the normal component E_z can be easily derived by $E_z = (-k_x/k_z)E_x + (-k_x/k_z)E_y$, where k_x, k_y and k_z are x, y, z components of the wave vector k. The tangential magnetic fields can also be derived by using

$$\begin{pmatrix} Z_0 H_x \\ Z_0 H_y \end{pmatrix} = T_{he} \begin{pmatrix} E_x \\ E_y \end{pmatrix} = \begin{pmatrix} -\dfrac{k_x k_y}{k_z k_0} & -\dfrac{k_y k_y}{k_z k_0} - \dfrac{k_z}{k_0} \\ \dfrac{k_z}{k_0} + \dfrac{k_x k_x}{k_z k_0} & \dfrac{k_x k_y}{k_z k_0} \end{pmatrix} \begin{pmatrix} E_x \\ E_y \end{pmatrix}, \tag{2}$$

where the matrix T_{he} denoted above transforms the electric fields into the corresponding magnetic fields. Here the magnetic fields are multiplied by the vacuum impedance, so they have the same units as the electric fields. The S matrix for the graphene can be derived by imposing the boundary conditions: 1) the tangential components of the electric field are continuous across the graphene; and 2) the discontinuity of the magnetic field at two sides of the graphene equals the surface current. Thus, we have

$$\begin{cases} \vec{E}_F^{(I)} + \vec{E}_B^{(I)} = \vec{E}_F^{(II)} + \vec{E}_B^{(II)}, \\ \vec{H}_F^{(I)} + \vec{H}_B^{(I)} - \vec{H}_F^{(II)} - \vec{H}_B^{(II)} = \\ \dfrac{1}{2} T^{\leftrightarrow}_{\sigma} \left(\vec{E}_B^{(I)} + \vec{E}_F^{(I)} + \vec{E}_B^{(II)} + \vec{E}_F^{(II)} \right), \end{cases} \tag{3}$$

where $\vec{E}_F^{(i)}/\vec{H}_F^{(i)}$ and $\vec{E}_B^{(i)}/\vec{H}_B^{(i)}$ are electric/magnetic waves propagating forward and backward in region i ($i = I$ or II, respectively indicate regions at two sides of graphene), respectively. Z_0 is the vacuum impedance. The matrix T is defined as

$$T = \begin{pmatrix} 0 & -1 \\ 1 & 0 \end{pmatrix}. \tag{4}$$

By solving eq. (3), we can derive the S matrix of the graphene. The S matrix for the whole system can be constructed by an iteration process.

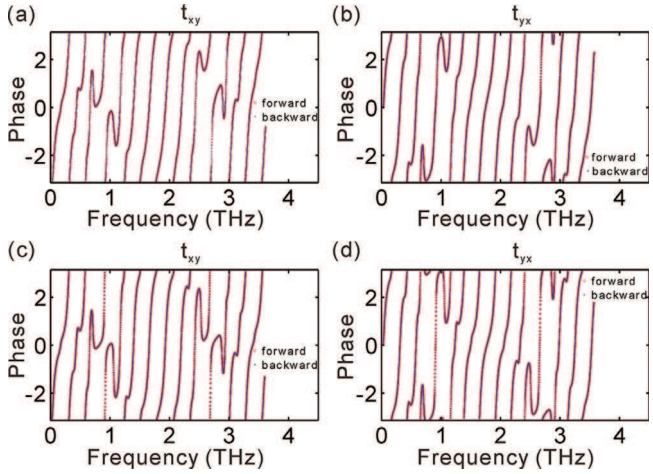

Fig. 2: (Colour on-line) Phases of the transmission coefficients t_{xy} and t_{yx} under $B = 6\,\text{tesla}$, $\mu = 0.25\,\text{eV}$ ((a), (b)), $B = 8\,\text{tesla}$, $\mu = 0.15\,\text{eV}$ ((c), (d)). Red circles and blue stars mark the phases of forward- and backward-propagating waves, respectively.

Jones matrices and non-reciprocal effect. – Non-reciprocity requires that the Jones matrix of the forward waves is not the transpose of the one for backward waves. Since the 2D conductivity tensor of graphene under magnetic field has rotation symmetry, it is impossible to tell whether the transmission is reciprocal or not only by investigating the absolute values of t_{xy} and t_{yx}, which are two off-diagonal elements of the Jones matrix. One should look into the phases. The phases of the transmission coefficients under specific magnetic field B and Fermi level μ are plotted in fig. 2. Figures 2(a), (b) are for $B = 6\,\text{tesla}$, $\mu = 0.25\,\text{eV}$ and figs. 2(c), (d) are for $B = 8\,\text{tesla}$, $\mu = 0.15\,\text{eV}$. We can see from fig. 2(a) and fig. 2(b) that the phase of t_{xy} for the forward waves (red circles in fig. 2(a)) is not the same as the phase for t_{yx} for backward waves (blue stars in fig. 2(b)). Similar conclusions can be found in fig. 2(c) and fig. 2(d). Such non-reciprocity originates from the asymmetry of the 2D conductivity tensor of graphene, which only depends on the direction of the magnetic field. Further investigations reveal that the difference of the phases of the off-diagonal terms in one direction is equal to π for all frequencies. This indicates that the Jones matrix of the structure under magnetic field has a form for both directions:

$$J = \begin{pmatrix} t & t' \\ -t' & t \end{pmatrix}, \tag{5}$$

where t and t' are the diagonal and off-diagonal terms of the Jones matrix, respectively. It can also be seen from fig. 2 that the Jones matrix has different values under different external magnetic fields and Fermi levels. So the non-reciprocal transmission coefficient of our structure can be tuned by changing either the external magnetic field or the Fermi level of graphene.

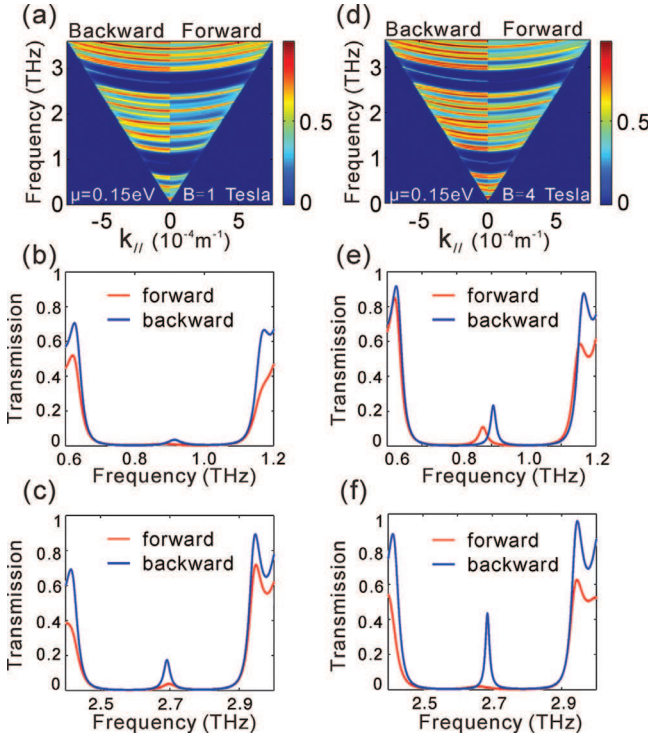

Fig. 3: (Colour on-line) Band structure (a), the first cavity mode (b) and the second cavity mode (c) for the case of $B = 1\,\text{T}$, $\mu = 0.15\,\text{eV}$. Band structure (d), the first cavity mode (e) and the second cavity mode (f) for the case of $B = 4\,\text{T}$, $\mu = 0.15\,\text{eV}$.

Tunable non-reciprocal band structures and transmission spectra. – In this section, we focus on the band structures and transmission spectra under the illumination of right-handed circularly polarized THz waves. The band structures are calculated by the transmission intensities under different incident angles. In the band gap, only the cavity modes can exist. The first cavity mode and the second cavity mode appear in the first and second band gaps, respectively. The calculation results are shown in fig. 3 and fig. 4. The corresponding magnetic-field intensities and Fermi levels are denoted therein. We can see from these figures that both band structures and transmission spectra are different for forward- and backward-propagating waves. In this design, backward-propagating waves have higher transmission than forward-propagating waves. Mode splitting and suppression may occur under specific conditions. For example, in fig. 4(f), the second cavity mode for forward-propagating waves is completely suppressed and no peak appears in the band gap while, for backward-propagating waves, the transmission peak is relatively high.

To further quantificationally measure the asymmetry, we define a contrast factor $f = (T_b - T_f)/(T_b + T_f)$, which equals zero if the spectra are symmetric and equals 1 if transmission of one direction is completely blocked. The contrast factors plotted as a function of magnetic

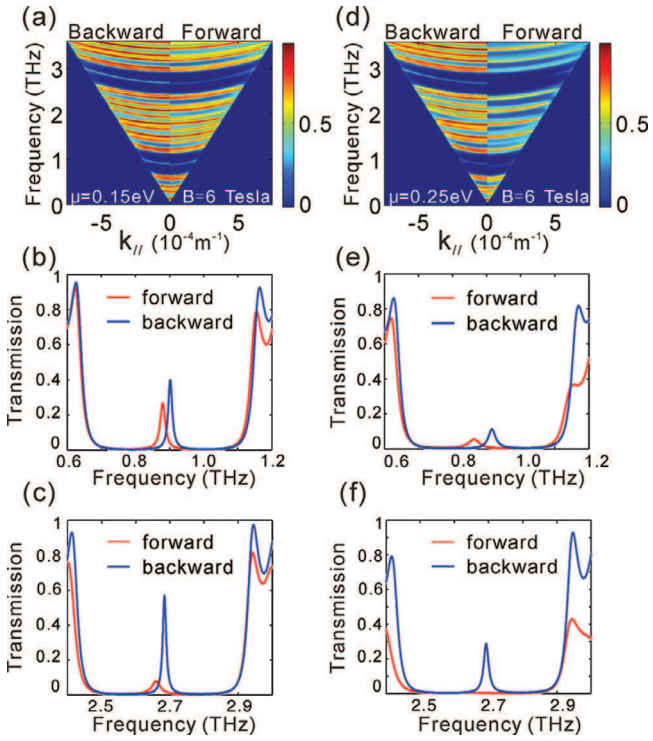

Fig. 4: (Colour on-line) Band structure (a), the first cavity mode (b) and the second cavity mode (c) for the case of $B = 6\,\mathrm{T}$, $\mu = 0.15\,\mathrm{eV}$. Band structure (d), the first cavity mode (e) and the second cavity mode (f) for the case of $B = 6\,\mathrm{T}$, $\mu = 0.25\,\mathrm{eV}$.

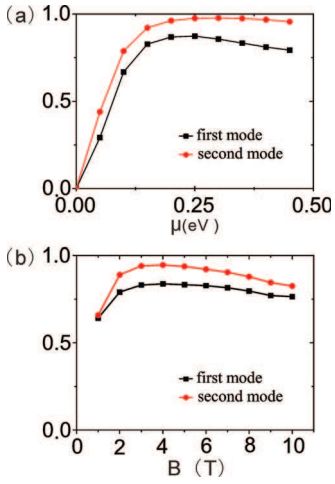

Fig. 5: (Colour on-line) (a) Contrast factor plotted as a function of the Fermi level when $B = 6\,\mathrm{T}$. (b) Contrast factor plotted as a function of the magnetic-field intensity when $\mu = 0.15\,\mathrm{eV}$.

field or Fermi level are shown in fig. 5. All the points are taken at the transmission peaks of backward waves. Figure 5(a) plots the contrast factor as a function of the Fermi level while keeping the magnetic field fixed at 6 T. As for $\mu = 0$, *i.e.*, pristine graphene without doping, there exists no significant non-reciprocal effect. For

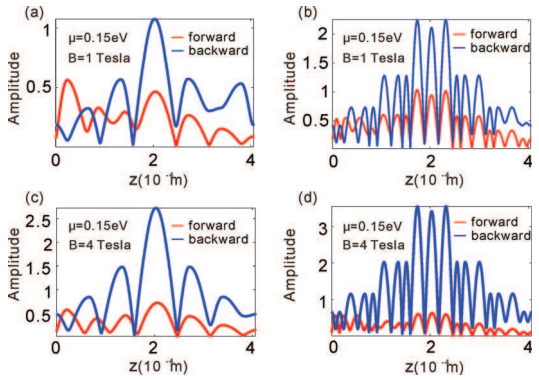

Fig. 6: (Colour on-line) Field amplitude distributions for (a) the first cavity mode and (b) the second cavity mode at the peak of the backward-propagating waves (blue curves) in figs. 3(b) and (c), respectively. Field amplitude distributions for (c) the first cavity mode and (d) the second cavity mode at the peak of the backward-propagating waves (blue curves) in figs. 3(e) and (f), respectively.

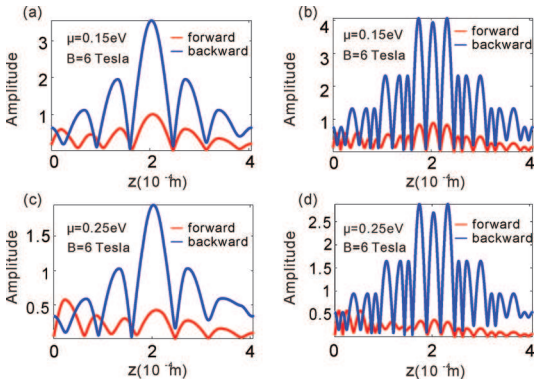

Fig. 7: (Colour on-line) Field amplitude distributions for (a) the first cavity mode and (b) the second cavity mode at the peaks of the backward-propagating waves (blue curves) in figs. 4(b) and (c), respectively. Field amplitude distributions for (c) the first cavity mode and (d) the second cavity mode at the peak of the backward-propagating waves (blue curves) in figs. 4(e) and (f), respectively.

graphene with doping, there exists an optimized Fermi level where the contrast factor reaches its maximum. Figure 5(b) shows the contrast factor as a function of the magnetic-field intensity while the Fermi level $\mu = 0.15$. The lowest magnetic field is set to be 1 tesla. One can see from the curves that for a fixed Fermi level, there also exists an optimized magnetic-field intensity that will maximize the contrast factor. Thus, tunable non-reciprocal band structure and transmission spectra can be achieved and optimized. Such non-reciprocity presented here may provide a way to achieve some THz one-way devices, such as isolators.

Non-reciprocal field distributions. – Since the S matrix involves an iteration process, it would be much more convenient for one to use the transfer matrix (T matrix) in field distribution calculations. Once the

fields at one of the ports (input or output ports) are known, the fields in the cavity structure can be derived by simple T matrix multiplication. Figure 6 and fig. 7 show field distributions under the same magnetic-field intensities and Fermi levels as in fig. 3 and fig. 4, respectively. All the field distributions are calculated at the frequencies of the transmission peaks of backward-propagating waves. At these frequencies, backward waves have higher field intensities than the forward waves, which is in accordance with the transmission spectra in fig. 3 and fig. 4 where backward waves dominate. Without graphene, the cavity mode is strictly symmetric and has perfect transmission [36,37]. In the presence of graphene, loss is unavoidable which will lower the transmission peak of the cavity mode and even break the symmetry of the field distribution. Under magnetic field and finite electron doping, non-reciprocal field distributions occur. This non-reciprocal field distribution has the same origin as the transmission spectra and the band structures, which is the asymmetry of the graphene conductivity tensor.

Non-reciprocal transmission through periodic stacks. – In order to enhance the non-reciprocal effect, we consider periodic photonic crystal stacks integrated with graphene. Here we put graphene in the building block to investigate the transmission of THz waves through periodic photonic crystal stacks. The conductivity of graphene is calculated under $B = 6\,\mathrm{T}$, $\mu = 0.4\,\mathrm{eV}$, mainly because the longitudinal and the Hall conductivities under this condition are both strong and close to each other, and thus it gives good contrast between forward and backward transmissions. Two kinds of building blocks are studied: one is that the graphene sheet is put on the surface of every dielectric slab (as shown in the inserts of figs. 8(a) and (b)); the other is that only one graphene sheet is inserted between two dielectric slabs (as shown in the inserts of figs. 8(c) and (d)). It is worthwhile to note that all the dielectric slabs have the same thicknesses as they do in the cavity. Figures 8(a) and (b) show the calculated transmissions of THz waves through five and ten periodic stacks with the first type of building block, respectively. Blue and red curves are transmissions in forward and backward directions, respectively. One can see that the contrast between forward and backward transmissions is close to 1. For instance, in fig. 8(b), the contrast is 0.9991 at 4 THz. Similar results are found in the periodic stacks with the second type of building block, as shown in figs. 8(c) and (d). This high-contrast non-reciprocal effect is attributed to two aspects: one is that graphene has strong conductivities; and the other is that the longitudinal and Hall conductivities are close to each other. Actually when a right-handed circularly polarized wave propagates through graphene, the conductivity is $\mathrm{Re}(\sigma_l) + \mathrm{Im}(\sigma_h)$ or $\mathrm{Re}(\sigma_l) - \mathrm{Im}(\sigma_h)$, which depends on the propagation direction. If the real part of the longitudinal conductivity is quite close to the imaginary part of the Hall conductivity, THz waves propagating through the

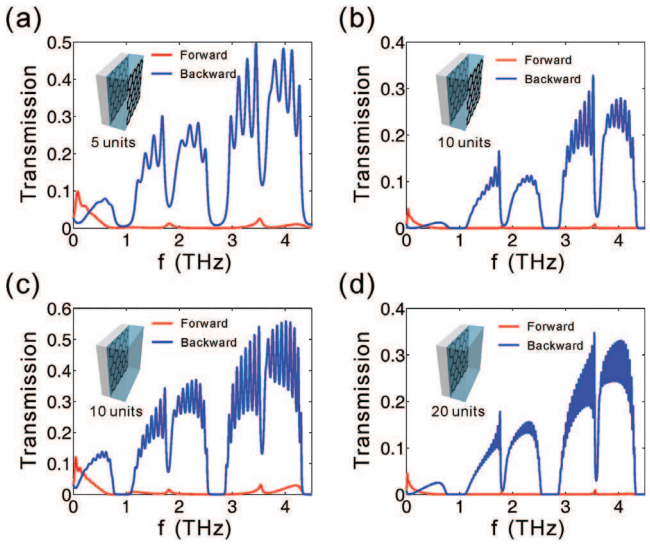

Fig. 8: (Colour on-line) Non-reciprocal transmission of THz waves through (a) 5 and (b) 10 periodic stacks of units. The insets show the corresponding units. There exist two graphene sheets in the unit. Non-reciprocal transmission of THz waves through (c) 10 and (d) 20 periodic stacks of units. The insets show the corresponding units. There exists only one graphene sheet in the unit.

structure will feel much stronger with conductivity in one direction ($\sigma = \mathrm{Re}(\sigma_l) + \mathrm{Im}(\sigma_h)$) than with that in the other direction ($\sigma = \mathrm{Re}(\sigma_l) - \mathrm{Im}(\sigma_h)$). This will lead to huge differences in both the loss and the reflection when the THz waves travel through the structure. Therefore, one can see in fig. 8 that high-contrast non-reciprocal transmission indeed exists in a rather broad frequency region.

Conclusions. – In this paper, we theoretically investigate tunable non-reciprocal transmission and band structure of terahertz waves through a photonic cavity integrated with graphene. Under magnetic field, 2D conductivity of graphene is asymmetric, which leads to the failure of reciprocity. As a result, circularly polarized waves propagating in two directions have different transmission spectra and field amplitude distributions. Such non-reciprocity at the level of material response enables us to design the photonic structure which can let a specific mode pass but its time-reversal counterpart stop. By tuning the external magnetic-field intensity or Fermi level of the graphene, one can tune the band structures, transmission spectra and field intensity distributions of the structure. Moreover, high-performance non-reciprocal features have been found in periodic photonic crystal stacks with graphene. Our investigations may provide a unique approach to guide THz waves and achieve potential applications on one-way devices (*e.g.* isolators) in the THz regime.

* * *

This work was supported by the MOST of China (Grants No. 2012CB921502 and 2010CB630705) and the NSFC (Grants No. 11034005, 11474157, and 61475070).

This article has been submitted by participants at the META'14 event in Singapore in May 2014. EPL supports the META series by providing annual sponsorship. The scientific content has been peer reviewed under the same guidelines and criteria as all other EPL letters.

REFERENCES

[1] De hoop A. T., *Appl. Sci. Res. B*, **8** (1959) 135.
[2] Potton R. J., *Rep. Prog. Phys.*, **67** (2004) 717.
[3] Aplet L. J. and Carson J. W., *Appl. Opt.*, **3** (1964) 544.
[4] Figotin A. and Vitebsky I., *Phys. Rev. E*, **63** (2001) 066609.
[5] Belov P. A., Tretyakov S. A. and Viitanen A. J., *Phys. Rev. E*, **66** (2002) 016608.
[6] Figotin A. and Vitebskiy I., *Phys. Rev. B*, **67** (2003) 165210.
[7] Yu Z., Wang Z. and Fan S., *Appl. Phys. Lett.*, **90** (2007) 121133.
[8] Wang Z., Chong Y. D., Joannopoulos John D. and Soljačić Marin, *Phys. Rev. Lett.*, **100** (2008) 013905.
[9] Takeda H. and John S., *Phys. Rev. A*, **78** (2008) 023804.
[10] Yu Z., Veronis G., Wang Z. and Fan S., *Phys. Rev. Lett.*, **100** (2008) 023902.
[11] Khanikaev A. B., Mousavi S. H., Shvets G. and Kivshar Y. S., *Phys. Rev. Lett.*, **105** (2010) 126804.
[12] He C., Lu M. H., Heng X., Feng L. and Chen Y. F., *Phys. Rev. B*, **83** (2011) 075117.
[13] Bliokh K. Y., Gredeskul S. A., Rajan P., Shadrivov I. V. and Kivshar Y. S., *Phys. Rev. B*, **85** (2012) 014205.
[14] Christofi A. and Stefanou N., *Phys. Rev. B*, **87** (2013) 115125.
[15] Davoyan A. R. and Engheta N., *Phys. Rev. Lett.*, **111** (2013) 047401.
[16] Dong H. Y., Wang J. and Cui T. J., *Phys. Rev. B*, **87** (2013) 045406.
[17] Chamanara N., Sounas D. and Caloz C., *Opt. Express*, **21** (2013) 11248.
[18] El-Ganainy R., Eisfeld A., Levy Miguel and Christodoulides D. N., *Appl. Phys. Lett.*, **103** (2013) 161105.
[19] Mazor Y. and Steinberg Ben Z., *Phys. Rev. Lett.*, **112** (2014) 153901.
[20] Degiron A. and Smith D. R., *Phys. Rev. E*, **89** (2014) 053203.
[21] Ra'di Y., Asadchy V. S. and Tretyakov S. A., *Phys. Rev. B*, **89** (2014) 075109.
[22] Wang Zheng, Chong Yidong, Joannopoulos J. D. and Soljačić Marin, *Nature*, **461** (2009) 772.
[23] Fu Jin-Xin, Liu Rong-Juan and Zhi-Yuan Li, *Appl. Phys. Lett.*, **97** (2010) 041112.
[24] Fu Jin-Xin, Liu Rong-Juan and Zhi-Yuan Li, *EPL*, **89** (2010) 64003.
[25] Fu Jin-Xin, Liu Rong-Juan, Gan Lin and Zhi-Yuan Li, *EPL*, **93** (2011) 24001.
[26] Fu Jin-Xin, Lian Jin, Liu Rong-Juan, Gan Lin and Zhi-Yuan Li, *Appl. Phys. Lett.*, **98** (2011) 211104.
[27] Bi L., Hu J., Jiang P., Kim D., Dionne G. F., Kimerling L. C. and Ross C. A., *Nat. Photon.*, **5** (2011) 758.
[28] Shalaby M., Peccianti M., Ozturk Y. and Morandotti R., *Nat. Commun.*, **4** (2013) 1558.
[29] Tocci M. D., Bloemer M. J., Scalora M., Dowling J. P. and Bowden C. M., *Appl. Phys. Lett.*, **66** (1995) 2324.
[30] Konotop V. V. and Kuzmiak V., *Phys. Rev. B*, **66** (2002) 235208.
[31] Novoselov K. S., Geim A. K., Morozov S. V., Jiang D., Zhang Y., Dubonos S. V., Grigorieva I. V. and Firsov A. A., *Science*, **306** (2004) 666.
[32] Grigorenko A. N., Polini M. and Novoselov K. S., *Nat. Photon.*, **6** (2012) 749.
[33] Bao Q. and Loh K. P., *ACS, Nano*, **6** (2012) 3677.
[34] Ferreira A., Viana-Gomes J., Bludov Y. V., Pereira V., Peres N. M. R. and Castro Neto A. H., *Phys. Rev. B*, **84** (2011) 235410.
[35] Fallahi A. and Perruisseau-Carrier J., *Phys. Rev. B*, **86** (2012) 195408.
[36] Peng R. W., Huang X. Q., Qiu F., Wang Mu, Hu A., Jiang S. S. and Mazzer M., *Appl. Phys. Lett.*, **80** (2002) 3063.
[37] Wang Z., Peng R. W., Qiu F., Huang X. Q., Wang Mu, Hu A., Jiang S. S. and Feng D., *Appl. Phys. Lett.*, **84** (2004) 3969.